Effect of the Metal–Support Interaction on the Catalytic Properties of Palladium for the Conversion of Difluorodichloromethane with Hydrogen: Comparison of Oxides and Fluorides as Supports

Bernard Coq,*,† François Figuéras,†,§ Serge Hub,‡ and Didier Tournigant†

Laboratoire de Materiaux Catalytiques et Catalyse en Chimie Organique, URA 418 CNRS; ENSCM, 8 rue de l'Ecole Normale, 34053 Montpellier Cedex, France and ELF ATOCHEM, Centre de Recherche Rhône-Alpes, rue Henri Moissan, BP 63, 69310 Pierre-Bénite, France

Received: December 21, 1994; In Final Form: May 9, 1995⊗

The reaction of difluorodichloromethane with hydrogen has been studied between 433 and 523 K and atmospheric pressure, over Pd catalysts supported on graphite and oxides or fluorides of Al, Ti, and Zr. In CF_2Cl_2 hydrogenation, CH_2F_2 and CH_4 represented more than 95% of the products. The catalytic properties of fluoride supported catalytsts did not undergo any change as a function of time. In contrast, Pd supported on oxides showed changes in selectivty during the first hours on stream. This was ascribed to the reaction of the oxide support with HF released during the reaction. Alumina and titania were nearly completely converted to the corresponding fluorides, but not zirconia. The selectivity to the desired product CH_2F_2 was 56% for Pd/graphite and reached 90% for Pd/ZrF_4. The kinetic study suggested that the selectivity was controlled by the bond strength between a carbene-like species CF_2 and the surface. The strength of this interaction is supposed to vary with electron availability at the Pd surface, and this hypothesis was then investigated by infrared spectroscopy using the adsorption of CO on Pd/Al_2O_3 and Pd/AlF_3. The results show that the morphology of the Pd particles was little affected by the support and that AlF_3-supported Pd becomes electron deficient, due to the strong Lewis acidity of the support. This effect is mainly a short-range effect which is better induced by supports made up of a mixture of fluorides, oxyfluorides, and hydroxyfluorides, rather than pure fluorides. Catalytic properties similar to those of Pd/AlF_3 and ZrF_4 can be simulated with Pd/graphite samples promoted with small amounts of aluminum or zirconium.

Introduction

Chlorofluorocarbons (CFCs) are charged with the seasonal depletion of the ozone layer above the poles in the stratosphere and for the greenhouse effect. As a result, there is an international agreement to freeze and then to reduce drastically the production and the release of these compounds. Owing to their chemical and physical properties, the CFCs were largely used as propellants for domestic use, solvents, blowing, and agent refrigerants. For the latter applications, hydrochlorofluorocarbons (HCFCs) and hydrofluorocarbons (HFCs) are excellent candidates as substitutes for CFCs.

The production of HCFCs and HFCs involves catalytic processes, namely fluorination of chloroalkanes over AlF_3 or Cr_2O_3 as catalysts, and hydrodechlorination of CFCs over metal catalysts, the latter presenting a major challenge for catalysis by metals.[1–3] Very few academic studies have dealt with this subject,[4–7] and the patent literature is scarce.[8–13] What emerges from these studies is that Pd, Ni, and Pt metals are most widely used and that Pd is preferred when fluoroalkanes are the desired products. Moreover, the role of the support is very important. It has to be resistant to hydrogen fluoride released in the course of the reaction and should be able to provide specific patterns of selectivity. It has been shown that the use of metal fluorides as supports allows better control of the extent of hydrodehalogenation.[6,7,10,12] Indeed, Kellner and Mallikarjuna Rao[10] claimed good yields, up to 76%, with 99% selectivity for the preparation of CH_2FCF_3 from $CHFClCF_3$ using Pd/AlF_3 as a catalyst. Coq et al.,[6] studying the conversion of CF_2Cl_2 at 473 K over Pd/graphite and Pd/AlF_3 catalysts of similar size of the Pd particles, reported a selectivity of 56.1% to CH_2F_2 on Pd/graphite but 80.3% on Pd/AlF_3. From this study it was shown that Pd/graphite underwent changes in selectivity during the first few hours on stream. The initial selectivity to CH_2F_2 on the fresh catalyst was around 70% but decreased upon fluorine deposition to reach 56% after 10 h on stream. The behavior of Pd/AlF_3 in the CF_2Cl_2 hydrogenation was merely reproduced when one started with a Pd/Al_2O_3 catalyst.[6] Actually, HF formed in the course of the reaction transformed Al_2O_3 to a mixture of aluminum fluoride and oxyfluoride phases, with a decrease of the surface area from 200 to 50 $m^2\ g^{-1}$.[6] It is noteworthy that the Pd/AlF_3 catalyst reported to be selective for the hydrodechlorination of CF_3CFCl_2 was prepared by fluorination of Al_2O_3 by HF/N_2 at 723 K.[10] The aim of the present work was to extend the aforementioned observations to other oxide supports and their fluoride analogues and to better understand the possible role of the fluoride and oxyfluoride phases. Different proposals were put forward to explain the promoting effect of AlF_3 on Pd to CH_2F_2 formation: (1) A geometrical effect based on the size and/or the morphology of the Pd particles; (2) an electronic effect at the metal/support interface; (3) a particular metal/support interaction between Pd and AlF_3.

It was suggested that an interaction, or a cooperation, of a particular kind between Pd particles and the AlF_3 carrier could occur.[6] When preparing Pd/AlF_3 catalysts, hydrogen fluoride was released during the final step of reduction, and AlF_x species ($x < 3$) would be formed at the periphery of the Pd particles. In the course of CF_2Cl_2 hydrogenation, these species would

§ Present address: Institut de Recherche sur la Catalyse du CNRS, 2 Av. A. Einstein, 69626 Villeurbanne.
† Laboratoire de Materiaux Catalytiques et Catalyse en Chimie Organique.
‡ ELF ATOCHEM.
* To whom the correspondence should be sent.
⊗ Abstract published in *Advance ACS Abstracts*, June 15, 1995.

0022-3654/95/2099-11159$09.00/0

TABLE 1: Main Characteristics of the Catalysts

catalyst	support	wt % Pd	reduction step temp (K)	duration (h)	gas	$(H/Pd)_{irr}$	mean particle size in nm determined by chem	TEM	XRD
PdGVIII	graphite	2.5	523	3	$H_2 + N_2$ (20 + 80)	0.15	6		22
Pd903	Al_2O_3	10	623	8	$H_2 + H_2O$ (97.5 + 2.5)	0.12	8	5.5	37
PdAlF3(I)	AlF_3	3.0	523	3	$H_2 + N_2$ (10 + 90)	0.10	10	12	10
PdAlF3(IV)	AlF_3	0.39	523	2	$H_2 + N_2$ (10 + 90)	0.17	6		8
PdTiO2(I)	TiO_2	3.0	523	3	$H_2 + N_2$ (10 + 90)	0.18	6		
PdTiO2(II)	TiO_2	3.0	773	1	H_2	0.08	12		
PdTiF3	TiF_3	3.2	523	1	$H_2 + N_2$ (10 + 90)	0.23	4.3	22	
PdZrO2(A)	ZrO_2 (amorphous)	3.1	523	3	$H_2 + N_2$ (10 + 90)	0.35	2.8		
PdZrO2(C)	ZrO_2 (crystalline)	3.0	523	1	$H_2 + N_2$ (10 + 90)	0.33	3.0		
PdZrF4(II)	ZrF_4	3.0	523	1	$H_2 + N_2$ (10 + 90)	0.05	19		

withdraw adsorbed fluorine atoms, hence scavenging the surface and protecting the Pd particles against diffusion of fluorine into the bulk. Absorbed fluorine in bulk Pd was thought to be responsible for the lack of CH_2F_2 selectivity. These hypotheses can be checked by studying the adsorption of CO by infrared spectroscopy, since these spectra can give information on the morphology and electron density at the metal surface.[14] For this purpose, and IR study of CO adsorption on Pd/Al_2O_3 and Pd/AlF_3 was carried out, and Pd supported on graphite was modified by the addition of aluminum and zirconium as promotors.

Experimental Section

Reactants. Hydrogen of high-purity grade (99.99%) was used for the catalytic experiments and hydrogen of ultrahigh purity (99.995%) for adsorption measurements. CF_2Cl_2 was obtained from ELF ATOCHEM (purity >99.95%). Palladium acetylacetonate ($Pd(acac)_2$, Aldrich, purity >99%), aluminum acetylacetonate ($Al(acac)_3$, Johnson Matthey) and zirconium acetylacetonate ($Zr(acac)_4$, Johnson Matthey) were used as precursors for the supported catalysts. The precursors were dissolved in dehydrated toluene (purity >99.5%). The carriers for the catalysts were γ-Al_2O_3 from Rhône-Poulenc (surface area 202 $m^2\ g^{-1}$), $AlF_3 \cdot 3H_2O$ from Rhône-Poulenc (surface area 75 $m^2\ g^{-1}$, purity >97%), TiO_2 from Degussa (surface area 40 $m^2\ g^{-1}$), TiF_3 from Johnson Matthey (surface area 23 $m^2\ g^{-1}$), ZrF_4 prepared in our laboratory, $ZrF_4 \cdot xH_2O$ from Aldrich (surface area 7 $m^2\ g^{-1}$) and graphite from LONZA (HSAG300, surface area 300 $m^2\ g^{-1}$). For simplicity, these supports will be referred to as AlF_3, TiF_3, and ZrF_4. High surface area zirconia was prepared by slow addition of $ZrOCl_2 \cdot 8H_2O$ (0.4 mol L^{-1}) and aqueous NH_4OH (2 mol L^{-1}) to excess water at a constant pH of 10.05. The precipitate formed was washed with high-purity water to remove chloride ions. The washed solid was dried at 383 K for 24 h and then crushed and sieved below 125 μm. This hydroxylated zirconia has a specific surface of 290 $m^2\ g^{-1}$. The preparation procedures are reported in detail elsewhere.[15] The amorphous form of zirconia was obtained by calcination at 573 K, whereas the crystalline zirconia (mainly tetragonal form) was obtained by calcination at 673 K for 3 h. The amorphous and crystalline supports are referred in the text as ZrO_2(A) and ZrO_2(C), respectively.

Preparation of Palladium Catalysts. The mono- and bimetallic Pd catalysts were prepared by dry impregnation or coimpregnation of the support with a solution of the precursors. The required amounts of the precursors were dissolved in toluene, then were brought into contact with the support at room temperature for several hours. Afterward, the solution was either evaporated or filtered. The solids were dried at 298 K under vacuum and then subjected to different thermal treatments involving both calcination and reduction steps. The parameters for preparing the catalysts are given in Table 1.

Characterization. The catalysts were characterized by hydrogen sorption, X-ray diffraction, and transmission electron microscopy. The chemisorption of hydrogen was carried out in a conventional volumetric apparatus, at 298 K in the 0−30 kPa pressure range. The sample was first reactivated in situ in a hydrogen stream at 523 K overnight and then evacuated to 1.2×10^{-4} Pa, at the same temperature, for 3 h. The double isotherm method proposed by Benson et al.[16] was used to measure the amount of hydrogen chemisorbed on the palladium surface as well as that absorbed as bulk β-palladium hydride. The first isotherm consists of both adsorbed and absorbed hydrogen; outgassing at room temperature for 30 min removes the absorbed hydrogen and completely destroys the β-PdH phase. The second (back-sorption) isotherm represents the amount of hydrogen absorbed into bulk palladium since hydrogen chemisorbed on the palladium surface has not been removed by evacuation at room temperature. The difference between the two curves represents the isotherm of adsorption of hydrogen. The extrapolated value at zero pressure was taken as the amount of irreversibly adsorbed hydrogen. Provided the surface stoichiometry of irreversibly adsorbed hydrogen is unity, we have the metal dispersion given by $D = (H/Pd)_{irr}$. The size of the metallic particles was checked by transmission electron microscopy using a JEOL 100CX microscope. X-ray diffraction patterns were recorded on a CGR Theta 60 instrument using monochromatized Cu $K\alpha_1$ radiation. Chemical compositions of the solids were determined by elemental analysis after dissolution, at the Service Central d'Analyse (CNRS, Solaize, France).

Table 1 summarizes the main characteristics of the catalysts. One can comment on the apparent disagreement between H_2 chemisorption and TEM on one hand and XRD on the other hand for determining the mean Pd particle size of Pd903, PdGVIII, and PdTiF3 samples. The larger values obtained from XRD for these samples are probably due to a broad particle size distribution, in which the small particles were not taken into account by the XRD analysis.

Fourier Transformed IR Spectra of Adsorbed CO. About 20 mg of the sample was pressed into a disk wafer with a 2 cm^2 surface. All catalyst treatments were performed in situ. The reactivation of the Pd catalyst is performed by three successive H_2 treatments at 473 K and 39.9 kPa for 1 h. Between each H_2 treatment the cell was evacuated. Thereafter, the IR spectra were recorded at room temperature with a Nicolet 60SX FTIR spectrometer at a resolution of 2 cm^{-1}. Generally, a scan number of 250 was chosen to improve the signal-to-noise ratio. CO (99.9%) was introduced to the IR cell, which has a volume of 366 cm^3, by successive pulses. The morphology of the Pd particles (proportion of different planes and defects) was estimated by treatment of the raw spectra using the method proposed by Binet et al.[14]

Catalytic Experiments. The reaction of difluorodichlo-

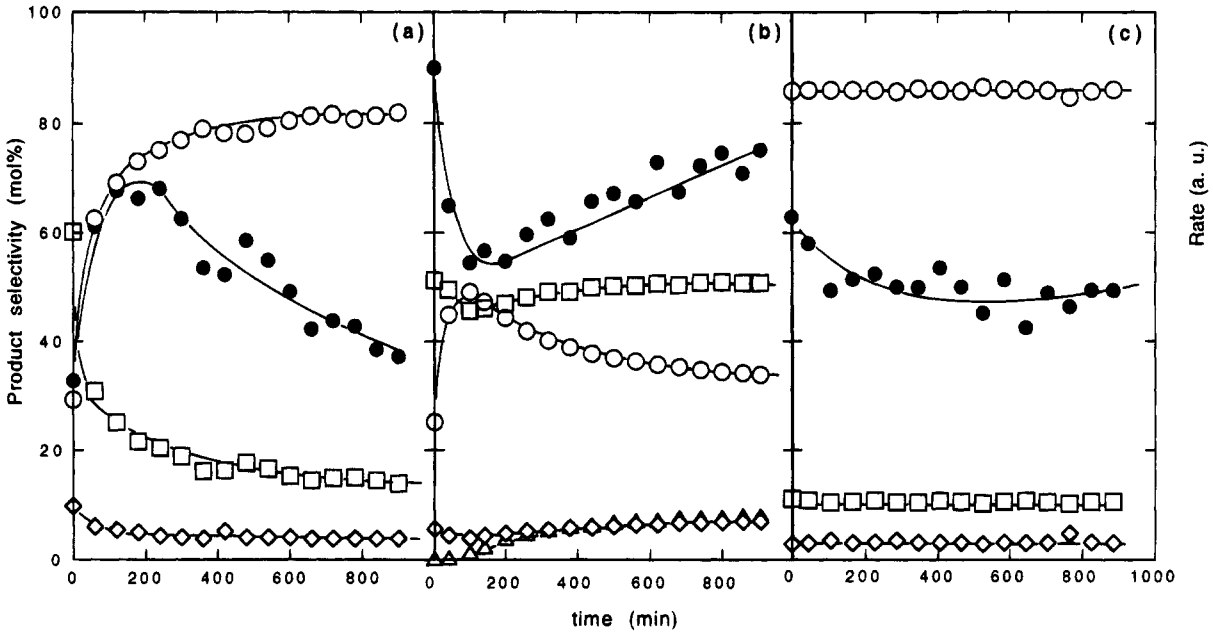

Figure 1. Product selectivities and reaction rate for the hydroconversion of CF_2Cl_2 over Pd catalysts as a function of time during the first hours under stream: (J) rate, (E) CH_2F_2, (G) CH_4, (Å) CHF_2Cl, (C) CF_2CF_2; (a) PdTiO2(I), (b) PdZrO2(C), (c) PdZrF4(II). T_R = 473 K.

romethane with hydrogen was carried out at atmospheric pressure in a microflow reactor. The flow rate of each reactant was controlled by a mass flow meter (ASM, Model Qualiflow AFC260). The effluents were analyzed by sampling on line to a gas chromatograph equipped with a J & W capillary column (30 m × 0.5 mm i.d., GSQ bonded polymer phase) and a thermal conductivity detector. The sample (500 mg) was reactivated in situ under flowing hydrogen at 523 K overnight. Usually Pd catalysts show changes of activity and selectivity with time on stream; therefore, a procedure was developed which allowed to reach constant catalytic properties. The procedure used for catalytic tests was as follows: (1) The reaction conditions were maintained at T_R = 473 K, CF_2Cl_2/H_2 = 0.30, space velocity = 2000 h^{-1} for 20 h. This step corresponds to passivation of the catalysts to reach constant activity and selectivity. (2) The reaction temperature was varied in the sequence 473, 433, 453, 413 K with CF_2Cl_2/H_2 = 0.3 and a space velocity between 2000 and 13 000 h^{-1}. (3) At a reaction temperature of 453 K, the feed composition was varied in the range $0.1 < CF_2Cl_2/H_2 < 4$ with a space velocity ranging from 2000 to 13 000 h^{-1} and alternating between high and low CF_2Cl_2/H_2 ratios. After the passivation period, the catalytic activity was reasonably stable as a function of time onstream, using these conditions. Activities are expressed both as moles of reactant converted per unit time per unit mass of catalyst and as turnover frequency (TOF) or number of molecules of reactant converted per surface metal atom per hour. Selectivities are defined as $S_i = 100C_i/\Sigma C_i$, where C_i is the molar concentration of the detected product i. Selectivities were measured at low conversions, usually less than 5%, in order to avoid secondary reactions. Thus they represent initial selectivities. Hydrogen chloride and hydrogen fluoride formed during the reaction were not taken into account as reaction products.

Results

In the course of CF_2Cl_2 reaction with hydrogen over supported Pd catalysts two main organic compounds are formed, namely, CH_2F_2 and CH_4, which usually represent more than 95% of the products. Besides these compounds, small amounts of CHF_2Cl (2–5%) were found. Traces lower than 1% of various compounds such as CH_3F, $CHFCl_2$, or CF_3Cl were also detected.

TABLE 2: Change of Catalytic Properties of Pd Catalysts during the Passivation Period; T_R = 473 K; $CF_2Cl_2/H_2 \approx 0.3$ mol/mol

	time on stream ≈ 10 min		time on stream ≈ 10 h	
sample	TOF (h^{-1})	CH_2F_2/CH_4	TOF (h^{-1})	CH_2F_2/CH_4
PdGVIII	73	2.1	72	1.1
Pd903	98	2.6[a]	61	3.7
PdAlF3(I)	138	4.9	166	3.6
PdAlF3(IV)	283	3.6	307	3.8
PdTiO2(I)	98	1.24[a]	71	4.93
PdTiO2(II)	221	2.59	123	5.41
PdTiF3	33	3.14	35	4.68
PdZrO2(A)	60	0.31	49	0.63
PdZrO2(C)	79	0.49	49	0.66
PdZrF4(II)	256	7.76	203	7.77

[a] In different test and at time zero, the ratio CH_2F_2/CH_4 was close to 0.5 for the two catalysts.

During the passivation period, different behaviors were observed:

(i) Pd catalysts supported on graphite, AlF_3, TiF_3, and ZrF_4 did not deactivate, while Pd catalysts supported on alumina, titania, or zirconia suffered a 20–50% activity loss.

(ii) The selectivity to methane increased with time onstream for Pd/graphite, remained constant for Pd on fluorides, but decreased for Pd on oxides (Figure 1 and Table 2).

XRD studies of the fresh and passivated Pd/Al_2O_3 catalysts showed that a large fraction of alumina was transformed to a mixture of aluminum fluoride and oxyfluoride phases.[6] This transformation, induced by HF released in the course of the reaction, was responsible for the increase in CH_2F_2 selectivity. It is worth noting that the Pd/AlF_3 catalyst claimed for the selective hydrodechlorination of CF_3CFCl_2 to CF_3CH_2F was prepared by fluorination of Al_2O_3 by HF at 723 K.[10] These changes in properties of the catalysts will be discussed further in detail.

At steady state, the catalytic properties were studied as a function of the reaction temperature and feed composition. Figure 2 illustrates the dependency of the reaction rate on the feed composition ($P(CF_2Cl_2)/P(H_2)$) for different Pd catalysts. The activity goes through a maximum and then decreases. This general behavior, observed for all the catalysts, led us to

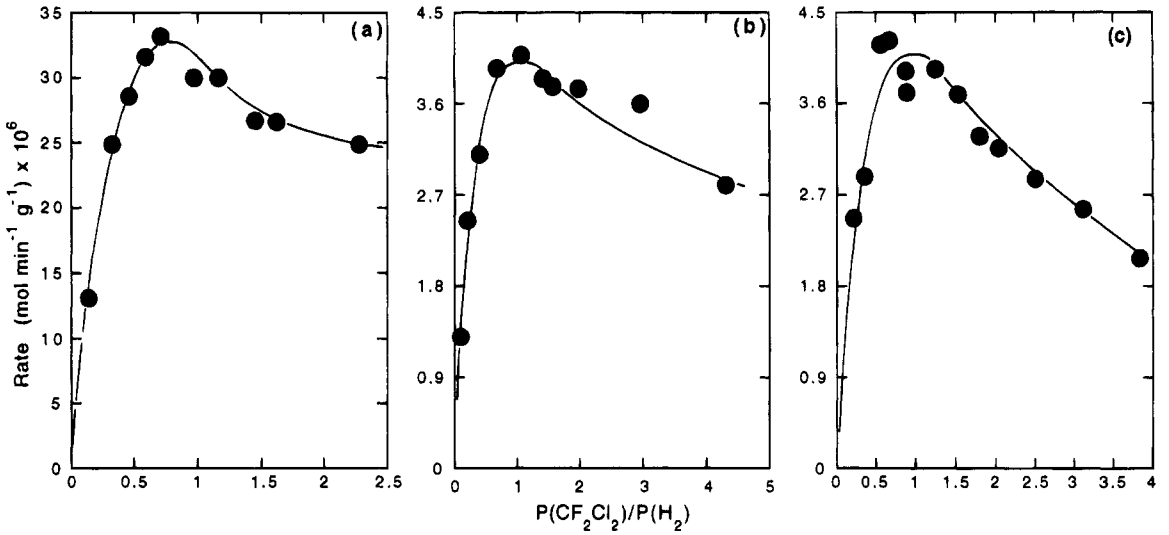

Figure 2. Reaction rate for the hydroconversion of CF_2Cl_2 over Pd catalysts as a function of feed composition; (a) PdZrF4(II), (b) PdZrF4(ATO), (c) PdAlG; T_R = 453 K.

speculate that hydrogen and CF_2Cl_2 compete for the same adsorption sites. By considering the findings in the literature and our experimental results, the following halogenation/dehalogenation mechanism was proposed:[6]

$$CF_2Cl_2 + H^* \rightarrow \text{products} + Cl^*,F^* \quad (1)$$

$$Cl^*,F^* + H_2 \rightarrow H^* + HCl,HF \quad (2)$$

where k_R is the rate constant for the halogenation of the Pd surface, and k_H the rate constant for the regeneration of the Pd surface; the asterisks refer to adsorbed species. The rate equation is

$$r = k_R P_R k_H P_H/(k_R P_R + k_H P_H) \quad (3)$$

assuming a first-order dependence with respect to CF_2Cl_2 and H_2 pressures for the halogenation and the regeneration of the Pd surface. Since the experiments were performed under atmospheric pressure (10^5 Pa), the rate law takes the form

$$r = 10^5 k_R k_H (P_R/P_H)/[k_R(P_R/P_H)^2 + (k_R + k_H)(P_R/P_H) + k_H] \quad (4)$$

When the P_R/P_H ratio varies from zero to infinity, the reaction rate goes through a maximum value r_m for $\delta r/\delta(P_R/P_H) = 0$. The two rate constants k_R and k_H can then be estimated from the values of the coordinates r_m and $(P_R/P_H)_m$ of this point

$$(P_R/P_H)_m = (k_H/k_R)^{0.5} \quad (5)$$

$$r_m = 10^5 k_H/[1 + (k_H/k_R)^{0.5}]^2 \quad (6)$$

The values of k_R and k_H were determined for all the catalysts and reported in Table 3. Regardless of the catalyst, it appears that the ratio between the two rate constants k_H and k_R does not change greatly, from 0.4 to 1.2, approximately. Thereby, the strength of interaction between the Pd surface and CF_2Cl_2 or H_2 is of the same order of magnitude and little affected by the nature of the support.

Finally, the values of the activation energies and the steady-state product selectivities are given in Table 4, for a feed composition of $P(CF_2Cl_2)/P(H_2) \approx 0.3-0.35$.

Discussion

By studying the reactivity of CHF_2Cl and CH_2F_2, we concluded in previous work that the hydrogenation of CF_2Cl_2 conforms to a modified rake scheme.[6] Chlorodifluoromethane would interact with the Pd surface by two parallel pathways to yield $*CF_2Cl$ or $*CF_2H$ adsorbed species. The latter is the more abundant species since in halomethanes, halogen–metal exchange is usually more rapid than hydrogen–metal exchange.[17] Moreover, only very little interconversion would exist between these species. In short, we found that the reactions favored are those allowing the removal of two halogen atoms before desorption from the surface: $CF_2Cl_2 \rightarrow CH_2F_2$, $CHF_2Cl \rightarrow CH_3F$, $CH_2F_2 \rightarrow CH_4$.[6] A similar behavior was observed in the conversion of CF_3CFCl_2 over Pd/C,[11] where only CF_3CH_2F and CF_3CH_3 were detected, in a constant ratio of 6, and the monohydrodechlorinated product CF_3CHFCl did not seem to

TABLE 3: Estimated Values of the Kinetic Parameters in the Halogenation/Dehalogenation Mechanism for the Conversion of CF_2Cl_2 at 453 K over Pd-Based Catalysts

catalyst	$(P_R/P_H)_m$	r_m[a]	k_H[b]	k_R[b]	TOF[c] (h^{-1})
PdGVIII	0.60	28	72	200	52.5
Pd903	1.1	90	397	328	47
PdAlF3(I)	0.9	74	267	330	165
PdAlF3(IV)	1.1	20	88	73	176
PdTiO2(I)	1.0	27.7	116	106	34
PdTiO2(II)	0.8	40.3	130	205	102
PdTiF3	0.7	19.7	59	109	17
PdZrO2(A)	0.9	35.3	127	157	21
PdZrO2(C)	0.8	54.8	181	270	36
PdZrF4(II)	0.7	33.2	96	196	135

[a] Expressed in (mole min^{-1} g^{-1}) × 10^6. [b] Expressed in (mole min^{-1} g^{-1}) × 10^{11}. [c] Specific activies calculated from r_m values at 453 K.

TABLE 4: Distribution of the Products and Activation Energies for Hydrogenation of CF_2Cl_2 at 453 K over Pd-Based Catalysts ($CF_2Cl_2/H_2 \approx 0.3-0.35$ mol/mol)

catalyst	conv (%)	E_a (kJ mol^{-1})	product selectivity (mol %)			
			CH_4	CH_2F_2	CHF_2Cl	others[a]
PdGVIII	5.9	61.5	40.5	56.1	1.7	1.7
Pd903	6.4	60.5	16.5	79.1	3.2	1.0
PdAlF3(I)	8.8	63.5	13.9	80.3	1.7	4.0
PdAlF3(IV)	2.0	75.0	17.2	78.4	4.1	0.3
PdTiO2(I)	2.1	84.5	16.8	81.0	2.2	
PdTiO2(II)	3.3	64.0	12.0	83.6	4.3	0.1
PdTiF3	2.4	65.5	13.1	81.8	4.9	0.2
PdZrO2(A)	2.2	82.5	39.0	52.2	5.0	3.7
PdZrO2(C)	6.2	69.5	48.9	31.4	8.7	10.8
PdZrF4(II)	3.5	74.0	9.6	86.0	3.8	0.1

[a] $CH_3F + CHFCl_2 + CF_3Cl$.

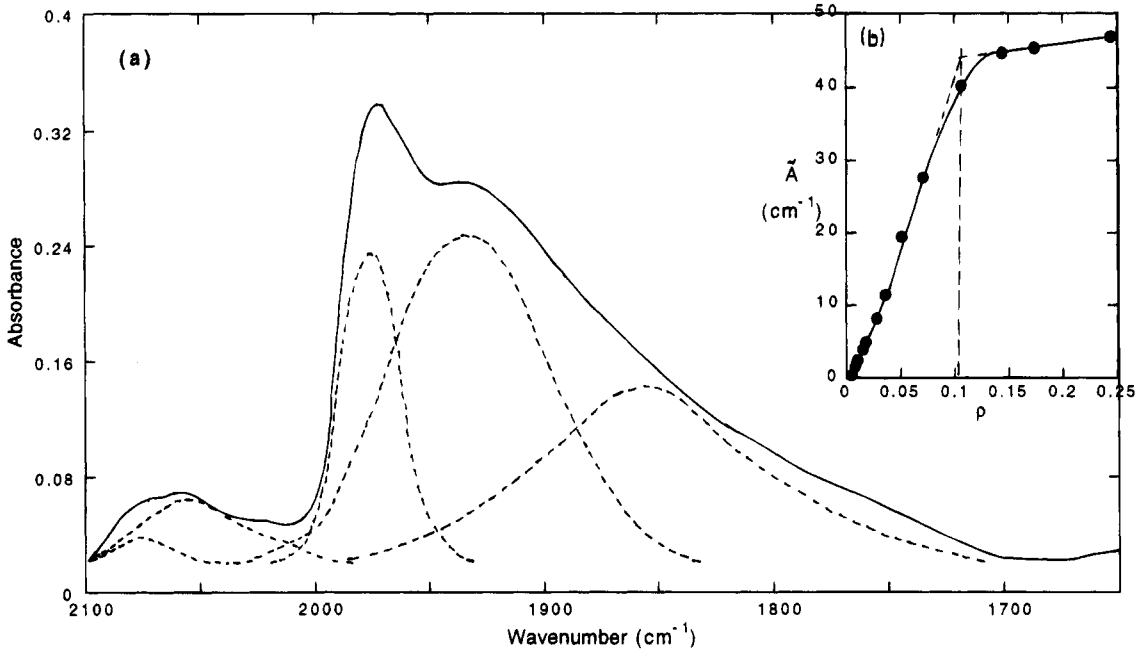

Figure 3. (a) Infrared spectrum of CO adsorption on Pd/Al_2O_3 (Pd903) catalyst at $\varrho = 0.144$, (– – – ~ ~) decomposition of the profile of the adsorption spectrum into ν_{CO} elementary bands; (b) plot of integrated absorbance $\tilde{A}$ as a function of ϱ, $\varrho = n_{CO}/N_{Pd}$.

desorb. Similarly, CH_3CHF_2 did not yield CH_3CH_2F but only C_2H_6.[18] In the hydrogenation of CF_2Cl_2, the most abundant surface intermediate would be the $*CF_2$ radical. The selectivity for the two main products, CH_2F_2 and CH_4, is mainly determined by the ratio between the desorption rate of $*CF_2$ assisted with hydrogen to give CH_2F_2 and the rate of the surface reaction leading to CH_4.

It emerges very clearly that the fluoride supports (AlF_3, ZrF_4, TiF_3) favor both the selectivity to CH_2F_2, which is generally larger than 80%, and the specific activities per surface Pd atoms. The fresh Pd catalysts supported on oxides exhibit lower CH_2F_2 selectivity, from 25% for Pd/ZrO_2 to 60% for Pd/Al_2O_3, but this selectivity increases for Pd/TiO_2 and Pd/Al_2O_3 in the course of the reaction. By contrast, the CH_2F_2 selectivity on $PdZrO_2$-(C) does not change very much, after a slight initial increase. As previously proposed,[6] these changes of catalytic properties come from the bulk transformation of alumina and titania to fluorinated phases by reaction with HF released in the catalytic process. This fluorination did not occur for crystalline zirconia. Indeed, X-ray diffraction patterns provided evidence that the tetragonal ZrO_2 phase was altered very little at the end of the reaction, and only traces of hydrated ZrF_4 phases appeared. By contrast, alumina is transformed to a large extent to AlF_3 and $AlF_{1.96}(OH)_{1.04}$ phases. TiO_2, which is a mixture of anatase (85%) and rutile (15%),[19] is transformed in part to $TiOF_2$. It is worth noting that only anatase underwent this bulk transformation, while rutile remained unmodified. Takita et al.[5b] reported partial bulk transformation during the hydrogenation of CF_3-$CFCl_2$ over Pd, Ni, and Pt supported on TiO_2.

The selectivity for the main products, CH_2F_2 and CH_4, is mainly determined by the ratio between the desorption rate of $*CF_2$ assisted with hydrogen to give CH_2F_2 and the rate of the surface reaction leading to CH_4.[6] The desorption of $*CF_2$, assisted by hydrogen, will be easier as the bond between $*CF_2$ and Pd will be weaker. In the metallocarbon $Pd{=}CF_2$ bond, the $*CF_2$ radical is electron withdrawing due to the inductive effect of fluorine atoms. Therefore, this metallocarbon bond will be weaker if Pd becomes electrodeficient. The electrodeficient character of the Pd surface can be checked by CO adsorption. Figures 3 and 4 present the IR spectra of adsorbed CO on Pd903 and PdAlF3(I) catalysts, respectively. These spectra were recorded at monolayer CO coverage estimated by the method proposed by Binet et al.[16] Several pulses of CO were introduced to the IR cell, and the total integrated absorbance $\tilde{A}$ was plotted as a function of ϱ ($\varrho = n_{CO}/N_{Pd}$, where n_{CO} is the number of moles of CO introduced into the cell and N_{Pd} is the number of moles of Pd atoms in the sample). These plots are presented in Figures 3b and 4b for the two samples. The intercept between the two extrapolated straight lines at low and high CO coverages gives the Pd dispersion.[14] The values of 0.11 and 0.08 found for Pd903 and PdAlF3(I), respectively, are in excellent agreement with the values derived from H_2 chemisorption (see Table 1). The IR spectra of CO adsorbed on Pd903 and PdAlF3(I) (Figures 3a and 4a) do not differ markedly. This is an indication of Pd particles being not very different in size and morphology. However, two interesting features differentiate the spectrum on PdAlF3(I) from that on Pd903: (i) a higher intensity of the low-frequency band; (ii) an upward shift of all the vibrational frequencies. To obtain more details on these features, the spectra were deconvoluted according to the procedures described by Binet et al.[14] (Figures 3a and 4a). Five elementary bands were extracted from the raw spectra. These bands, labeled A_1, A_2, B, C, and D in a decreasing wavenumber order were assigned to the following adsorbed CO species:[14] (i) A_1 and A_2 bands correspond to linearly adsorbed CO on low coordination sites, such as edges and corners; (ii) the band B corresponds to bridged CO in C_{2v} symmetry on (100) faces; (iii) C and D bands correspond to bridged CO in C_{2v} and C_{3v} symmetry on (111) faces, respectively. The deconvoluted spectra allow us to estimate the proportion of (111) faces, (100) faces, and low coordination sites in the two catalysts (Table 5). What emerges from these spectra is that the main difference between Pd903 and PdAlF3-(I) is a higher density of the low coordination sites and the (100) faces on the latter. This means that the average coordination number of surface Pd atoms will be lower on PdAlF3(I). On the other hand, the wavenumbers for A_1, A_2, B, C, and D bands on Pd903 are in good agreement with the values found on a $Pd/\alpha Al_2O_3$ catalyst of similar dispersion (D = 0.12).[14] In a previous study on Pd/AlF_3 catalysts[6] we found that decreasing the size of Pd particles, which results in a higher proportion of the low coordination sites, decreases the CH_2F_2 selectivity. We

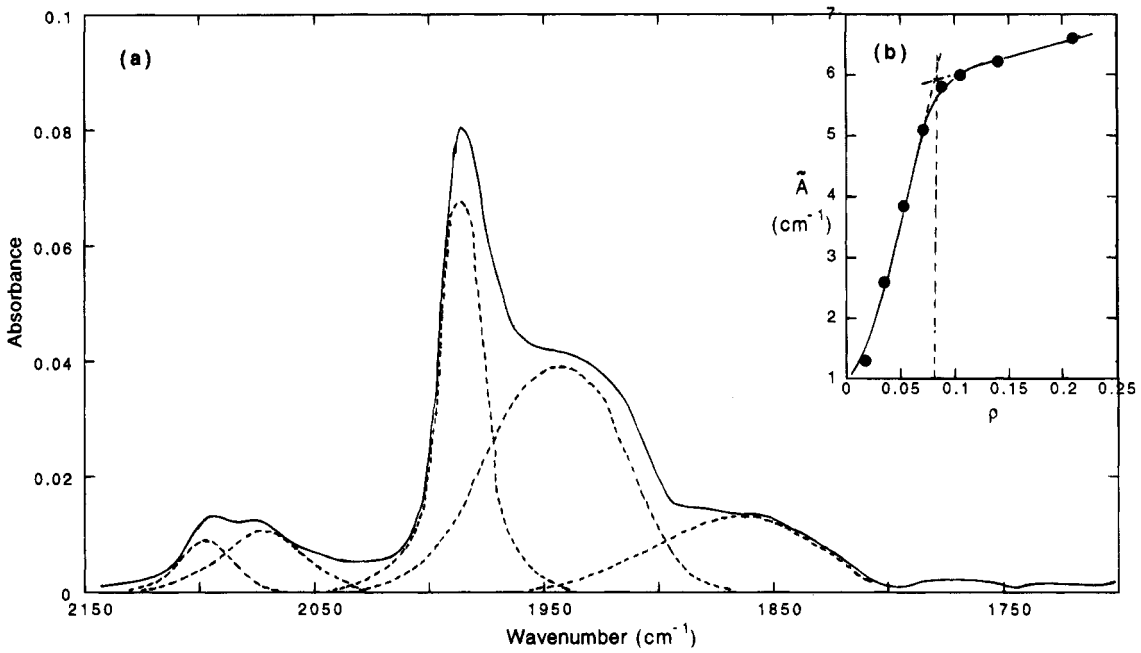

Figure 4. (a) Infra-Red spectrum of CO adsorption on Pd/AlF_3 (PdAlF3(I)) catalyst at $\varrho = 0.144$, (− − − ~ ~) decomposition of the profile of the adsorption spectrum into ν_{CO} elementary bands; (b) plot of integrated absorbance $\tilde{A}$ as a function of ϱ, $\varrho = n_{CO}/N_{Pd}$.

TABLE 5: Proportion (%) of Defects and Faces on Pd Particles Supported on Al_2O_3 (Pd903) and AlF_3 (PdAlF3(I)) Catalysts

catalyst	defects (edges, corners, etc.)	(100) face	(111) face
Pd903	7	16	77
PdAlF3(I)	11	29	60

can therefore conclude that the higher CH_2F_2 selectivity found on PdAlF3(I) compared to Pd903 is not the result of a morphology change of Pd particles since a higher density of low coordination sites exists on the former.

The second feature shown by the IR spectra is the upward shift (10−20 cm^{-1}) of all vibrational frequencies for CO adsorbed on PdAlF3(I). There is a universal agreement that the higher the stretching frequency of the C−O bond, the lower the bond strength between the carbon and the metal atoms.[20,21] That behavior is usually ascribed to a lower back donation of d electron in the $2\pi^*$ antibonding orbital of the CO bond. In the present work, when the support is changed from Al_2O_3 to AlF_3, the shift of the ν_{CO} bands by 10−20 cm^{-1} may be related to the variation of the electron density at the Pd atoms, this electron density is lower when Pd is supported by AlF_3. This behavior is certainly due to the strong Lewis acidity of AlF_3.[22] A similar shift of C−O stretching frequency was reported when comparing Pd/HY and Pd/MgO.[23]

To identify more precisely if the effect of fluoride supports on the enhancement of CH_2F_2 is a short-range or long-range one, we prepared graphite-supported PdAl and PdZr "bimetallic" catalysts, labeled PdAlGr and PdZrGr, respectively. The bimetallic catalysts were prepared by coimpregnation of graphite with $Pd(acac)_2$ and $Al(acac)_3$ or $Zr(acac)_4$ in toluene solution. After evaporation of the solvent, the solids were activated following the same procedure as used for the PdGVIII catalyst. The resulting solids were then evaluated in the hydrogenation of CF_2Cl_2. At steady state, the behavior of the bimetallic PdAlGr catalyst agrees very nicely with that of Pd supported on AlF_3, both for catalytic properties (Figure 5) and for kinetics (Figure 2c). However, the more interesting point deals with the passivation period. In the passivation step, during the first 10 h on stream, the behavior of PdAlGr and PdZrGr greatly differs from that of the pure Pd on graphite catalyst. On the latter, the CH_2F_2 selectivity decreases from 66% to 50% (Table 2). By contrast, the CH_2F_2 selectivity on PdAlGr and PdZrGr increases (Figure 5). This fact is particularly clear on PdAlGr since the CH_2F_2 selectivity, equal to 55% at the beginning of the reaction, reaches a value of 78% after 10 h on stream. A parallel decrease of CH_4 selectivity is then observed. At the end of the passivation period the patterns of selectivity on PdAlGr and Pd/Al_2O_3 are very close. This "bimetallic" effect is really specific to Al and Zr since the addition of Co, Ag, Fe, or K did not increase at all the CH_2F_2 selectivity.[24] We suspect that Al, and to a lower extent Zr, were fluorinated in PdAlGr and PdZrGr catalysts; the intimate contact between Pd and AlF_x, ZrF_x species ($x \leq 3, 4$) being responsible for the decrease of CF_2Cl_2 hydrodefluorination. However, it was impossible to detect the presence of any kind of AlF_x or ZrF_x species in these catalysts, due to the low amount of aluminum and zirconium, 0.49 and 1.52 wt %, respectively for 1.8 wt% Pd.

In a previous study,[6] we found that the decrease of CH_2F_2 selectivity on Pd black and Pd/graphite during the passivation step was correlated with a shift of the Pd(111) and Pd(220) lines of Pd to smaller diffraction angles. This showed a 3% increase of the interplanar distances, accounted for by the diffusion of fluorine into the bulk of Pd particles. Since this shift of Pd diffraction lines did not appear with Pd/AlF_3 catalysts, we concluded that adsorbed AlF_x species on Pd surface protected Pd against diffusion of halide species, which are responsible for the loss of CH_2F_2 selectivity.[6] However, this proposition no longer remains valid since in the passivation of PdAlGr and PdZrGr, Pd diffraction lines are shifted to smaller angles but the CH_2F_2 selectivity increases at the same time. Therefore, the key point for preserving CH_2F_2 selectivity on Pd catalysts is the presence of AlF_x, ZrF_x, or TiF_x moities ($x \leq 3, 4$) in the vicinity, or on, the Pd particles. The diffusion of fluorine into the bulk of Pd particles is of lesser importance.

The two studies of IR spectroscopy of adsorbed CO and on the catalytic properties of bimetallic PdAl and PdZr catalysts, have shown that there is probably not a long range effect of fluoride supports on Pd. A short range effect of AlF_x, TiF_x, or ZrF_x at the periphery, or on, the Pd particles is very likely. Indeed, a very small amount of fluoride species is sufficient to

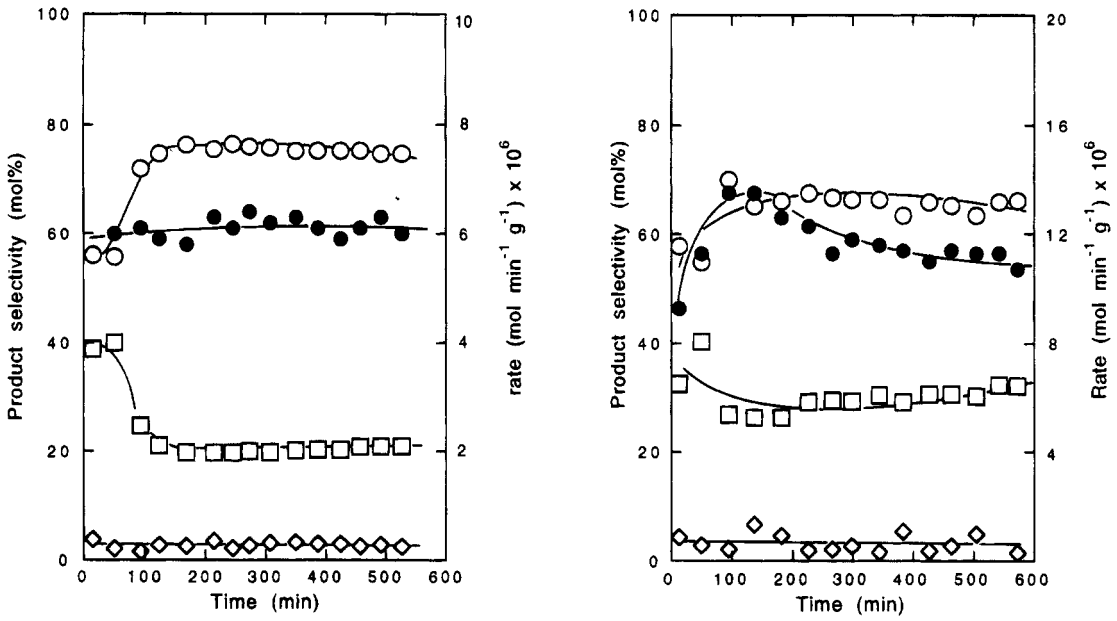

Figure 5. Product selectivities and reaction rate for the hydroconversion of CF_2Cl_2 over graphite-supported bimetallic Pd catalysts as a function of time during the first hours under stream: (J) rate, (E) CH_2F_2, (G) CH_4, (Å) CHF_2Cl; (a) PdAlGr (b) PdZrGr. T_R = 473 K.

TABLE 6: Influence of the Temperature of Treatment under N_2 of "ZrF_4" Support ($ZrF_4 \cdot H_2O$ + $ZrF_4 \cdot HF \cdot 3H_2O$ + $ZrF_4 \cdot HF \cdot 4H_2O$) on the Occurrence of Different "Fluoride Zr Phases" before and after $Pd(acac)_2$ Deposition and Reduction at 523 K

temp of treatment under N_2	373 K	523 K	673 K
phases present after N_2 treatment	$ZrF_4 \cdot H_2O$ (tetragonal) amorphous	ZrF_4 (monoclinic) amorphous	ZrF_4 (monoclinic) $Zr_7F_{10}O_9$ (orthorhombic) $ZrF_{2.67}O_{0.67}$ (cubic) amorphous
phases present after $Pd(acac)_2$ deposition and reduction at 523 K	$ZrF_4 \cdot H_2O$ (tetragonal) $Zr_7F_{10}O_9$ (orthorhombic) amorphous	ZrF_4 (monoclinic) γ-ZrF_4 $ZrF_4 \cdot H_2O$ (tetragonal) amorphous	ZrF_4 (monoclinic) γ-ZrF_4 $Zr_7F_{10}O_9$ (orthorhombic) $ZrF_{2.67}O_{0.67}$ (cubic) amorphous
label of the catalyst	PdZrF4(VI)	PdZrF4(V)	PdZrF4(IV)

initiate good CH_2F_2 selectivity. Thus, on PdAlGr catalysts the main changes in catalytic properties occurred during the first 100 min on stream where the CH_2F_2 selectivity increased from 55% to 73% (Figure 5a). Assuming that all the hydrogen fluoride formed reacted with aluminum to yield AlF_3, a simple calculation shows that 100 min is just enough to transform all the aluminum (0.49 wt %) the catalyst contains. On the other hand, following the same reasoning, only 1% of TiO_2 would be transformed to TiF_3 during the first 50 min on stream (Figure 1a).

In agreement with these comments, the origin of the enhancement in CH_2F_2 selectivity on fluoride-supported Pd catalysts is more complex than proposed and described above.[6] We recall that we speculated that AlF_x species would scavenge from Pd the fluorine species responsible for the loss of CH_2F_2 selectivity on Pd/graphite and Pd black catalysts. The IR study of adsorbed CO has shown that υ_{CO} of monocarbonyl species is shifted to higher frequencies by 10−20 cm^{-1} for Pd/AlF_3 compared to Pd/Al_2O_3. This means that palladium is very likely more electron deficient when supported on AlF_3 due to the strong Lewis acidity of this material.[22] In conclusion, we can guess that an electronic effect (electron withdrawing effect) of AlF_x,-TiF_x, or ZrF_x in the vicinity of Pd particles (mixed site) would be the key factor to reach high CH_2F_2 selectivity.

We have seen previously that in Pd/AlF_3,TiF_3,ZrF_4, and Pd/Al_2O_3, TiO_2, and ZrO_2 after reaction, the "fluoride" supports are actually a complex mixture in which we have identified fluoride, hydrated fluoride, oxyfluoride, and hydroxyfluoride phases. Even if we have concluded above that the effect of fluoride support can be mainly understood as a short-range effect, the question about the possible effect, in a second-order range, of the bulk nature of the support can be asked. Pd/ZrF_4 was found as the most selective catalyst for CH_2F_2 formation, we decided thus to delineate the effect of the different "fluoride" phases of zirconium. Various "ZrF_4" materials were obtained using two different methods:

(i) By thermal treatments of the commercial ZrF_4 under N_2 at various temperatures. The different phases identified by XRD before and after the deposition of $Pd(acac)_2$ are presented in Table 6. The raw ZrF_4 material was treated at three different temperatures under N_2. The solids loses between 11−30% weight in this treatment, accounted for H_2O (about 75%) and HF (about 25%). Whatever the thermal treatment, a mixture of fluoride, hydrated fluoride, oxyfluoride, and hydroxyfluoride phases constituted the support of the final catalyst.

(ii) By fluorination of the high surface zirconia (290 m^2 g^{-1}) with HF . The fluorination was carried out in a fixed-bed reactor. Zirconia (10 cm^3) was first dried under a N_2 flow (50 cm^3 s^{-1}) at 573 K for 3 h. The dried ZrO_2 was then fluorinated first at 473 K under diluted HF (N_2/HF 50/50, flow 100 cm^3 s^{-1}) and then under pure HF at 573 K for 18 h. The resulting solid contained only α- and γ-ZrF_4 phases and exhibited a surface area of 5.5 m^2 g^{-1}. This material did not undergo any change during the deposition and activation of the Pd phase.

The catalyst exhibiting the lowest CH_2F_2 selectivity is that which is free of hydrated fluoride, oxyfluoride, and hydroxyfluoride phases, i.e., PdZrF4(ATO) (Table 7). By contrast, all the catalysts that are very selective for CH_2F_2 formation contain

TABLE 7: Catalytic Properties for the Hydrogenation of CF_2Cl_2 at 453 K over "ZrF_4"-Supported Pd Catalysts ($CF_2Cl_2/H_2 \approx 0.3-0.35$ mol/mol)

catalyst	H/Pd	TOF (h^{-1})	E_a (kJ mol^{-1})	product selectivity (mol %)			
				CH_4	CH_2F_2	CHF_2Cl	others[a]
PdZrF4(II)	0.05	102	74.0	9.6	86.0	3.8	0.1
PdZrF4(IV)			69.5	5.8	90.2	2.7	1.3
PdZrF4(V)	0.015	65	73.0	7.2	89.1	2.2	1.5
PdZrF4(VI)	0.02	19	70.0	7.1	91.6		1.3
PdZrF4(ATO)	0.015	69	80.0	14.2	78.6	5.5	1.6

[a] $CH_3F + CHFCl_2 + CF_3Cl$.

some hydrated oxy- or hydroxyfluoride phases. It is worth noting that Kellner et al.[25] suggested that the Re/AlF_3 catalyst selective for hydrodechlorination of CFCs contained oxy- and hydroxyfluoride phases. The same was true for a Pd/Al_2O_3 partially fluorinated as reported by Oshio et al.[26] However, we have not yet any rational explanation for the specific properties introduced by oxygen-containing fluoride phases. It is possible that these phases make the formation and/or migration of substoichiometric AlF_x or ZrF_x moieties at the vicinity of the Pd particles easier.

During the kinetic study, the selectivity patterns were recorded as a function of reaction temperature and feed composition. In general, CH_4 selectivity increases with temperature due to the higher activation energy of the surface reaction leading to methane.[6] As regards the feed composition, there is no major effect of that parameter on the selectivity trends exhibited by the fluoride-supported Pd catalysts.

Conclusion

The conversion under hydrogen of CF_2Cl_2 over Pd-supported on graphite, Al_2O_3, TiO_2, ZrO_2, AlF_3, TiF_3, and ZrF_4 yields two main products, CH_2F_2 and CH_4. The selectivity of the reaction is highly dependent on the nature of the support. The use of fluoride supports allows one to reach up to 91% CH_2F_2 selectivity, whereas on Pd/graphite the CH_2F_2 selectivity is 56%. Al_2O_3 and TiO_2 supports are transformed in part to AlF_3 and TiF_3 due to HF released in the course of the reaction. ZrO_2 does not undergo this bulk reaction. The Pd/ZrF_4 catalysts most selective to CH_2F_2 are those containing a mixture of fluoride, oxyfluoride, and hydroxyfluoride phases. The promotion of CH_2F_2 selectivity is probably initiated by the formation of substoichiometric AlF_x, TiF_x, and ZrF_x moieties at the vicinity, or on, the Pd particles. Due to the strong Lewis acidity of these fluoride species Pd sites become electron deficient. The lower electron density of Pd favors the desorption of $*CF_2$, the most abundant surface intermediate, and hence the selectivity to CH_2F_2

Acknowledgment. The authors gratefully thank C. Binet (Caen, France) for helpful discussion and IR experiments and H. Ozkan (University of Ohio) for editing the manuscript.

References and Notes

(1) Rabo, J. A. New Frontiers in Catalysis. *Proceedings 10th International Congress on Catalysis*, Guczi, L., Solymosi, F., Tétényi, P., Eds.; Akadémiai Kiado: Budapest, 1993; Vol. A, p 1.
(2) Armor, J. N. *Appl. Catal. B: Environmental* **1992**, *1*, 221.
(3) Manzer, L. E, Mallikarjuna Rao, V. N., Adv. Catal. **1992**, *39*, 329.
(4) Gervasutti, C.; Marangoni, L.; Parra, W. *J. Fluorine Chem.* **1981**, *19*, 1.
(5) (a) Takita, Y.; Yamada, H.; Hashida, M.; Ishihara, T. *Chem. Lett.* **1990**, 715. (b) Takita, Y.; Yamada, H.; Ishihara, T.; Mizuhara, Y. *Nippon Kagaku Kaishi* **1991**, 584.
(6) Coq, B.; Cognion, J. M.; Figuéras, F.; Tournigant, D. *J. Catal.* **1993**, *141*, 21.
(7) Takita, Y.; Yamada, H.; Yoshida, K.; Hashida, M.; Mizuhara, Y.; Ishihara, T. *Nippon Kagaku Kaishi* **1992**, *1*, 9.
(8) Darragh, J. I. British Patent 1,578,933, 1980.
(9) Gervasutti, C. Eur. Patent 0,253,410, 1987.
(10) Kellner, C. S.; Mallikarjuna Rao, V. N. U.S. Patent 4,873,381, 1989.
(11) Mallikarjuna Rao, V. N. PCT Int. Appl. WO 92 12,113, 1992.
(12) Kellner, C. S.; Mallikarjuna Rao, V. N.; Weigert, F. J. U.S. Patent 5,146,018, 1993.
(13) Seki, E.; Aoyama, H.; Nakada, T.; Koyama, S. PCT Int. Appl. WO 93 10,067, 1993.
(14) Binet, C.; Jadi, A.; Lavalley, J. C. *J. Chim. Phys.* **1989**, *86*, 451.
(15) El Alami D. Ph.D. Thesis, Montpellier, 1993.
(16) Benson, J. L.; Hwang, H. S., Boudart, M. *J. Catal. 30*, 146. 1973.
(17) March, J. Advanced Organic Chemistry, 3rd ed.; John Wiley and Sons: New York, 1985; p 561.
(18) Witt, S. D.; Wu, E. C.; Loh, K. L.; Tang, Y. N. *J. Catal.* **1981**, *71*, 270.
(19) Haller, G. L.; Resasco, D. E. *Adv. Catal.*, Academic Press: **1989**, *36*, 173.
(20) Cotton, F. A.; Wilkinson, G. *Advanced Inorganic Chemistry*; Interscience: New York, 1962; p 616.
(21) Poiblanc, R.; Bigorgne, M. *Bull. Soc. Chem.* **1962**, 1301.
(22) Hess, A., Kemnitz, E. *J. Catal.* **1994**, *149*, 449.
(23) Figuéras, F.; Gomez, R.; Primet, M. *Molecular Sieves*; Meier, W. M., Uytterhoeven, J. B., Eds.; Advanced in Chemistry Series 121, American Chemical Society: Washington, DC, 1973; p 480.
(24) Coq, B.; Hub, S.; Figuéras, F.; Tournigant, D. *Appl. Catal. A*, **1993**, *101*, 41.
(25) Kellner, C. S.; Mallikarjuna Rao, V. N. W.O. 90/08 748, 1990.
(26) Oshio, H.; Mishumi, S.; Yagii, K.; Yoshikawa, S.; Murata, K. F.R. 2,631,959 A1, 1989.

JP9433719